

# REPORT DOCUMENTATION PAGE

Form Approved  
OMB No. 0704-0188

Public reporting burden for this collection of information is estimated to average 1 hour per response, including the time for reviewing instructions, searching existing data sources, gathering and maintaining the data needed, and completing and reviewing this collection of information. Send comments regarding this burden estimate or any other aspect of this collection of information, including suggestions for reducing this burden to Department of Defense, Washington Headquarters Services, Directorate for Information Operations and Reports (0704-0188), 1215 Jefferson Davis Highway, Suite 1204, Arlington, VA 22202-4302. Respondents should be aware that notwithstanding any other provision of law, no person shall be subject to any penalty for failing to comply with a collection of information if it does not display a currently valid OMB control number. PLEASE DO NOT RETURN YOUR FORM TO THE ABOVE ADDRESS.

1. REPORT DATE (DD-MM-YYYY)		2. REPORT TYPE Technical Papers		3. DATES COVERED (From - To)	
4. TITLE AND SUBTITLE				5a. CONTRACT NUMBER	
				5b. GRANT NUMBER	
				5c. PROGRAM ELEMENT NUMBER	
6. AUTHOR(S)				5d. PROJECT NUMBER 2302	
				5e. TASK NUMBER MIG 2	
				5f. WORK UNIT NUMBER	
7. PERFORMING ORGANIZATION NAME(S) AND ADDRESS(ES) Air Force Research Laboratory (AFMC) AFRL/PRS 5 Pollux Drive Edwards AFB CA 93524-7048				8. PERFORMING ORGANIZATION REPORT	
9. SPONSORING / MONITORING AGENCY NAME(S) AND ADDRESS(ES) Air Force Research Laboratory (AFMC) AFRL/PRS 5 Pollux Drive Edwards AFB CA 93524-7048				10. SPONSOR/MONITOR'S ACRONYM(S)	
				11. SPONSOR/MONITOR'S NUMBER(S)	
12. DISTRIBUTION / AVAILABILITY STATEMENT  Approved for public release; distribution unlimited.					
13. SUPPLEMENTARY NOTES					
14. ABSTRACT					
15. SUBJECT TERMS					
16. SECURITY CLASSIFICATION OF:			17. LIMITATION OF ABSTRACT  A	18. NUMBER OF PAGES	19a. NAME OF RESPONSIBLE PERSON Leilani Richardson
a. REPORT Unclassified	b. ABSTRACT Unclassified	c. THIS PAGE Unclassified			19b. TELEPHONE NUMBER (include area code) (661) 275-5015

7  
2  
1  
5  
1  
1

36 separate files are enclosed

G2

MEMORANDUM FOR PR (Contractor/In-House Publication)

FROM: PROI (TI) (STINFO)

16 Jun 2000

SUBJECT: Authorization for Release of Technical Information, Control Number: **AFRL-PR-ED-TP-2000-130**  
Y. Wei, C.L. Chow (University of Michigan); C.T. Liu (AFRL/PRSM), "Damage Analysis for Mixed Mode Crack Initiation"

**International Journal on Computational Science**  
**(Submission Deadline: 30 June 2000)**

**(Statement A)**

1. This request has been reviewed by the Foreign Disclosure Office for: a.) appropriateness of distribution statement, b.) military/national critical technology, c.) export controls or distribution restrictions, d.) appropriateness for release to a foreign nation, and e.) technical sensitivity and/or economic sensitivity.

Comments: \_\_\_\_\_  
\_\_\_\_\_  
\_\_\_\_\_

Signature \_\_\_\_\_ Date \_\_\_\_\_

2. This request has been reviewed by the Public Affairs Office for: a.) appropriateness for public release and/or b) possible higher headquarters review.

Comments: \_\_\_\_\_  
\_\_\_\_\_  
\_\_\_\_\_

Signature \_\_\_\_\_ Date \_\_\_\_\_

3. This request has been reviewed by the STINFO for: a.) changes if approved as amended, b.) appropriateness of distribution statement, c.) military/national critical technology, d.) economic sensitivity, e.) parallel review completed if required, and f.) format and completion of meeting clearance form if required

Comments: \_\_\_\_\_  
\_\_\_\_\_  
\_\_\_\_\_

Signature \_\_\_\_\_ Date \_\_\_\_\_

4. This request has been reviewed by PR for: a.) technical accuracy, b.) appropriateness for audience, c.) appropriateness of distribution statement, d.) technical sensitivity and economic sensitivity, e.) military/national critical technology, and f.) data rights and patentability

Comments: \_\_\_\_\_  
\_\_\_\_\_

APPROVED/APPROVED AS AMENDED/DISAPPROVED

\_\_\_\_\_  
LESLIE. S. PERKINS, Ph.D (Date)  
Staff Scientist  
Propulsion Directorate

20021119 137

# Damage Analysis for Mixed Mode Crack Initiation

Y. Wei and C.L. Chow

Department of Mechanical Engineering  
University of Michigan-Dearborn  
Dearborn, MI 48128, USA

C.T. Liu

Air Force Research Laboratory  
Edwards AFB, CA 93524-7680

## Summary

The paper presents a numerical simulation for mixed mode crack initiation based on the concepts of damage mechanics. A model with two scalar damage variables is introduced for characterization of damage in a material element. Then a tangent modulus tensor is derived for damage-coupled constitutive equations. A failure criterion is developed with the concept of damage accumulation not only to identify the location of damaged element with the crack initiation angle but also to determine the critical load for mixed mode fracture. The damage model developed is incorporated in a general-purpose finite element program ABAQUA through its UMAT subroutine. The finite element program is then used to perform numerical simulation for pre-cracked specimens under monotonic tensile loading. The thin plates are made of aluminum alloy and particulate composite embedded with a crack of inclined angle  $\beta=0^\circ, 30^\circ, 45^\circ$  and  $60^\circ$  for mixed mode fracture analysis. The predicted crack initiation loads and the angles of crack initiation agree well with the test results.

## Introduction

Most conventional approaches for mixed mode fracture prediction are based on the theory of fracture mechanics. The fracture parameters, such as the stress intensity factor  $K_C$  and the strain energy release rate  $G_C$  for brittle materials, the J-integral and COD for ductile materials, have been widely applied to conduct fracture analysis of engineering components containing a macro-crack. However, an important mechanism of failure in the materials is attributed to the presence of micro-cracks/voids. These micro-defects result in changes of mechanical property in the form of material degradation due to initiation, growth and coalescence of these micro-defects. Complete avoidance of such material damage is not realistic, especially for stress analysis at a crack tip. In addition, research results have cast doubts on the validity of the J-integral and COD as intrinsic material properties for ductile fracture, which by definition should be independent of geometry and loading history [1-3].

The material damage has been successfully characterized with the theory of damage mechanics first introduced by Kachanov [4] and later developed by many researchers [5,6]. With the introduction of averaging macro-variables (damage variables), the deterioration of materials as a result of the nucleation and growth of distributed material micro-defects can be determined quantitatively. Chow and Wang developed an anisotropic model which has been successfully applied to analyze mixed mode crack initiation and propagation of aluminum alloy

2024-T3 [7-9]. The model is based on a second-order damage tensor. Considerable computing time is however required for the FEM analysis on the transformation between local coordinate system and principal damage coordinate system. For the sake of computing efficiency, Chow and Wei have recently proposed an isotropic damage model with two scalars [10]. This paper is intended to present an investigation on the application of the proposed damage model to characterize ductile behavior of two materials, including damage-coupled constitutive equations, finite element formulation and ductile fracture of mixed mode crack.

### Damage-Coupled Constitutive Equations

The gradual deterioration of the material under service due to nucleation and growth of micro-cracks or defects can be characterized with an internal state variable known as damage variable [5]. Chow and Wei have recently developed a two-scalar damage model to evaluate damage accumulation under both monotonic and cyclic loading [10]. This section provides a brief description of the model required in the following sections for the development of finite element formulation.

Following the damage mechanics theory, the effective stress is defined as

$$\bar{\sigma} = \mathbf{M}(\mathbf{D}) : \sigma \quad (1)$$

where  $\sigma$  is the true stress tensor,  $\mathbf{D}$  is the damage tensor and  $\mathbf{M}(\mathbf{D})$  is the damage effect tensor which can be expressed as

$$\mathbf{M}(\mathbf{D}) = \frac{1}{1-D} \begin{bmatrix} 1 & \mu & \mu & 0 & 0 & 0 \\ \mu & 1 & \mu & 0 & 0 & 0 \\ \mu & \mu & 1 & 0 & 0 & 0 \\ 0 & 0 & 0 & 1-\mu & 0 & 0 \\ 0 & 0 & 0 & 0 & 1-\mu & 0 \\ 0 & 0 & 0 & 0 & 0 & 1-\mu \end{bmatrix} \quad (2)$$

$D$  and  $\mu$  are two scalar variables to characterize damage accumulation in materials. The thermodynamic conjugate forces of the damage variables  $D$  and  $\mu$ , known as the damage energy release rate, can be derived from the Helmholtz free energy  $\psi$  as

$$\begin{aligned} Y_D &= -\rho \frac{\partial \psi}{\partial D} = -\frac{1}{1-D} \sigma^T : \mathbf{C}^{-1} : \sigma \\ Y_\mu &= -\rho \frac{\partial \psi}{\partial \mu} = -\frac{1}{1-D} \sigma^T : \mathbf{Z} : \sigma \end{aligned} \quad (3)$$

where  $\mathbf{C}$  is the elastic tensor for damaged materials

$$\mathbf{C}^{-1} = \frac{1}{E} \begin{bmatrix} 1 & -\nu & -\nu & 0 & 0 & 0 \\ -\nu & 1 & -\nu & 0 & 0 & 0 \\ -\nu & -\nu & 1 & 0 & 0 & 0 \\ 0 & 0 & 0 & 2(1+\nu) & 0 & 0 \\ 0 & 0 & 0 & 0 & 2(1+\nu) & 0 \\ 0 & 0 & 0 & 0 & 0 & 2(1+\nu) \end{bmatrix} \quad (4)$$

The tensor  $\mathbf{Z}$  can be expressed as

$$\mathbf{Z} = \frac{1}{E_0(1-D)} \begin{bmatrix} z_1 & z_2 & z_2 & 0 & 0 & 0 \\ z_2 & z_1 & z_2 & 0 & 0 & 0 \\ z_2 & z_2 & z_1 & 0 & 0 & 0 \\ 0 & 0 & 0 & 2(z_1 - z_2) & 0 & 0 \\ 0 & 0 & 0 & 0 & 2(z_1 - z_2) & 0 \\ 0 & 0 & 0 & 0 & 0 & 2(z_1 - z_2) \end{bmatrix} \quad (5)$$

$$z_1 = 2\mu(1 - \nu_0) - 2\nu_0$$

$$z_2 = (1 + \mu)(1 - \nu_0) - 2\mu\nu_0$$

$E$  and  $\nu$  are respectively the effective Young's modulus and effective Poisson's ratio for damaged material. The relationships between  $E$  and  $\nu$  and the damage variables  $D$  and  $\mu$  are established as

$$E = \frac{E_0(1-D)^2}{1 - 4\nu_0\mu + 2(1 - \nu_0)\mu^2} \quad \nu = \frac{\nu_0 - 2(1 - \nu_0)\mu - (1 - 3\nu_0)\mu^2}{1 - 4\nu_0\mu + 2(1 - \nu_0)\mu^2} \quad (6)$$

$E_0$  and  $\nu_0$  are the values of Young's modulus and Poisson's ratio for intact or undamaged material.

The elastic law of damaged material can be expressed in the effective stress-effective strain space as

$$\bar{\sigma} = \mathbf{C}_0 : \bar{\epsilon}^e \quad (7)$$

where  $\mathbf{C}_0$  is the initial elastic tensor for undamaged material. The yield surface is postulated with the concept of the effective stress as

$$F_p(\bar{\sigma}, R) = \sigma_p - [R_0 + R(p)] = 0 \quad (8)$$

where  $\sigma_p$  is the effective equivalent stress

$$\sigma_p = \left\{ \frac{1}{2} \bar{\sigma}^T : \mathbf{H}_0 : \bar{\sigma} \right\}^{1/2} = \frac{1-\mu}{1-D} \sigma_{eq} \quad (9)$$

$\sigma_{eq}$  is the Von-Mises equivalent stress,  $\mathbf{H}_0$  is the plastic characteristic tensor for undamaged material,  $R_0$  is the yield stress,  $p$  is the effective equivalent plastic strain, and  $R$  is the strain hardening threshold. The constitutive equations of plasticity for damaged materials are accordingly derived in the effective stress-effective strain space as

$$d\bar{\varepsilon}^p = \lambda_p \frac{\partial F_p}{\partial \bar{\sigma}} \quad dp = \lambda_p \frac{\partial F_p}{\partial (-R)} = \lambda_p \quad (10)$$

The plastic damage surface is formulated with the thermodynamic conjugate forces of the plastic damage variables as

$$F_d(Y_d, B) = Y_d - [B_0 + B(w)] = 0 \quad (11)$$

where  $Y_d$  is the equivalent damage energy release rate postulated as

$$Y_d = \left\{ \frac{1}{2} (Y_D^2 + \gamma Y_\mu^2) \right\}^{1/2} \quad (12)$$

$B_0$  is the initial plastic damage threshold,  $B$  is the plastic damage hardening,  $w$  is the overall plastic-damage, and  $\gamma$  is the damage evolution coefficient. The plastic damage evolution equations are

$$\begin{aligned} dD &= -\lambda_d \frac{\partial F_d}{\partial Y_D} = -\frac{\lambda_d Y_D}{2Y_d} & d\mu &= -\lambda_d \frac{\partial F_d}{\partial Y_\mu} = -\frac{\lambda_d \gamma Y_\mu}{2Y_d} \\ dw &= -\lambda_d \frac{\partial F_d}{\partial B} = \lambda_d \end{aligned} \quad (13)$$

where  $\lambda_d$  is the Lagrange multiplier.

### Finite Element Formulation

The proposed damage model is discretized and coded in the user subroutine UMAT of a finite element package known as ABAQUS (Version 5.8). The implementation aims at providing a tool for numerical analysis based on the proposed damage model and validating the model by comparing its predictions with experimental measurements. The procedure is similar in principle to the conventional FEM analysis, except that the tangent modulus tensor is coupled with the damage variables. The formulation of the tangent modulus tensor is derived as follows.

The total elastic strain shown in equation (7) can be alternatively written as

$$d\bar{\sigma} = \mathbf{C}_0 : d\bar{\varepsilon}^e = \mathbf{C}_0 : d\bar{\varepsilon} - \mathbf{C}_0 : d\bar{\varepsilon}^p \quad (14)$$

Multiplying the above equation by  $\left(\frac{\partial F_p}{\partial \bar{\sigma}}\right)^T$  yields

$$\left(\frac{\partial F_p}{\partial \bar{\sigma}}\right)^T : d\bar{\sigma} = \left(\frac{\partial F_p}{\partial \bar{\sigma}}\right)^T : \mathbf{C}_0 : d\bar{\varepsilon} - \left(\frac{\partial F_p}{\partial \bar{\sigma}}\right)^T : \mathbf{C}_0 : d\bar{\varepsilon}^p \quad (15)$$

From the yield surface equation (8), we have

$$\begin{aligned} dF_p(\bar{\sigma}, R) &= \left(\frac{\partial F_p}{\partial \bar{\sigma}}\right)^T : d\bar{\sigma} - \frac{dR}{dp} dp = 0 \\ \left(\frac{\partial F_p}{\partial \bar{\sigma}}\right)^T : d\bar{\sigma} &= \frac{dR}{dp} dp \end{aligned} \quad (16)$$

Substituting the equations (10) and (16) into (15), we obtain the incremental plastic strain as

$$dp = \frac{\left(\frac{\partial F_p}{\partial \bar{\sigma}}\right)^T : \mathbf{C}_0 : d\bar{\varepsilon}}{\frac{dR}{dp} + \left(\frac{\partial F_p}{\partial \bar{\sigma}}\right)^T : \mathbf{C}_0 : \frac{\partial F_p}{\partial \bar{\sigma}}} \quad (17)$$

Thus the relationship between  $d\bar{\sigma}$  and  $d\bar{\varepsilon}$  is obtained with equations (10), (14) and (17) as

$$d\bar{\sigma} = \mathbf{C}_0^{ep} : d\bar{\varepsilon} \quad (18)$$

where  $\mathbf{C}_0^{ep}$  is the instantaneous tangent modulus tensor expressed as

$$\mathbf{C}_0^{ep} = \mathbf{C}_0 - \frac{(\mathbf{C}_0 : \frac{\partial F_p}{\partial \bar{\sigma}}) : (\mathbf{C}_0 : \frac{\partial F_p}{\partial \bar{\sigma}})^T}{\frac{dR}{dp} + (\frac{\partial F_p}{\partial \bar{\sigma}})^T : \mathbf{C}_0 : (\frac{\partial F_p}{\partial \bar{\sigma}})} \quad (19)$$

From the definition of yield surface in equation (8),

$$\frac{\partial F_p}{\partial \bar{\sigma}} = \frac{l}{2\sigma_p} \mathbf{H}_0 : \bar{\sigma} = \frac{l}{2\sigma_p} \mathbf{H}_0 : \mathbf{M} : \sigma \quad (20)$$

Substituting it into equation (19), the tensor  $\mathbf{C}_0^{ep}$  can be derived with equation (9) as

$$\mathbf{C}_0^{ep} = \mathbf{C}_0 - \frac{(\mathbf{C}_0 : \mathbf{H}_0 : \boldsymbol{\sigma}) : (\mathbf{C}_0 : \mathbf{H}_0 : \boldsymbol{\sigma})^T}{4\sigma_{eq}^2 \frac{dR}{dp} + (\mathbf{H}_0 : \boldsymbol{\sigma})^T : \mathbf{C}_0 : (\mathbf{H}_0 : \boldsymbol{\sigma})} \quad (21)$$

The above formulation of the instantaneous tangent modulus in equation (19) or (21) is expressed in terms of the incremental effective stress and strain in equation (18). However a finite element program such as ABAQUS is written in the true stress-true strain space. Therefore, it is necessary to transform equation (18) to the conventional stress-strain space as:

$$d\boldsymbol{\sigma} = \mathbf{C}^{ep} : d\boldsymbol{\varepsilon} \quad (22)$$

where  $\mathbf{C}^{ep}$  is the effective instantaneous tangent modulus tensor in true stress-true strain space which can be derived and described in the following section.

From the definition of effective stress in equation (1),

$$d\bar{\boldsymbol{\sigma}} = d\mathbf{M} : \boldsymbol{\sigma} + \mathbf{M} : d\boldsymbol{\sigma} \quad (23)$$

The relationships between the effective and true elastic strain and plastic strain are

$$\bar{\boldsymbol{\varepsilon}}^e = \mathbf{M}^{T,-1} : \boldsymbol{\varepsilon}^e \quad d\bar{\boldsymbol{\varepsilon}}^p = \mathbf{M}^{T,-1} : d\boldsymbol{\varepsilon}^p \quad (24)$$

Therefore, the effective strain is derived as

$$\begin{aligned} d\bar{\boldsymbol{\varepsilon}} &= d\bar{\boldsymbol{\varepsilon}}^e + d\bar{\boldsymbol{\varepsilon}}^p = \mathbf{M}^{T,-1} : d\boldsymbol{\varepsilon} + d\mathbf{M}^{T,-1} : \boldsymbol{\varepsilon}^e \\ &= \mathbf{M}^{T,-1} : d\boldsymbol{\varepsilon} - d\mathbf{M}^{T,-1} : \mathbf{M}^{T,-1} : \boldsymbol{\varepsilon}^e \end{aligned} \quad (25)$$

With the plastic damage evolution laws in equation (13),  $d\mathbf{M}$  can be expressed as

$$d\mathbf{M} = \frac{\partial \mathbf{M}}{\partial D} dD + \frac{\partial \mathbf{M}}{\partial \mu} d\mu = -\left(\frac{\partial \mathbf{M}}{\partial D} \frac{\partial F_d}{\partial Y_D} + \frac{\partial \mathbf{M}}{\partial \mu} \frac{\partial F_d}{\partial Y_\mu}\right) dw \quad (26)$$

From the plastic damage surface expressed in equation (11)

$$dF_d = \frac{\partial F_d}{\partial Y_D} dY_D + \frac{\partial F_d}{\partial Y_\mu} dY_\mu - \frac{dB}{dw} dw = 0 \quad (27)$$

Then, with the formulae

$$\begin{aligned}
dY_D &= \left( \frac{\partial Y_D}{\partial \sigma} \right)^T : d\sigma + \frac{\partial Y_D}{\partial D} dD + \frac{\partial Y_D}{\partial \mu} d\mu \\
&= \left( \frac{\partial Y_D}{\partial \sigma} \right)^T : d\sigma - \left( \frac{\partial Y_D}{\partial D} \frac{\partial F_d}{\partial Y_D} + \frac{\partial Y_D}{\partial \mu} \frac{\partial F_d}{\partial Y_\mu} \right) dw \\
dY_\mu &= \left( \frac{\partial Y_\mu}{\partial \sigma} \right)^T : d\sigma + \frac{\partial Y_\mu}{\partial D} dD + \frac{\partial Y_\mu}{\partial \mu} d\mu \\
&= \left( \frac{\partial Y_\mu}{\partial \sigma} \right)^T : d\sigma - \left( \frac{\partial Y_\mu}{\partial D} \frac{\partial F_d}{\partial Y_D} + \frac{\partial Y_\mu}{\partial \mu} \frac{\partial F_d}{\partial Y_\mu} \right) dw
\end{aligned} \tag{28}$$

Equation (27) becomes

$$\begin{aligned}
dw &= \mathbf{T} : d\sigma \\
\mathbf{T} &= \frac{\frac{\partial F_d}{\partial Y_D} \left( \frac{\partial Y_D}{\partial \sigma} \right)^T + \frac{\partial F_d}{\partial Y_\mu} \left( \frac{\partial Y_\mu}{\partial \sigma} \right)^T}{\frac{dB}{dw} + \frac{\partial Y_D}{\partial D} \left( \frac{\partial F_d}{\partial Y_D} \right)^2 + \left( \frac{\partial Y_D}{\partial \mu} + \frac{\partial Y_\mu}{\partial D} \right) \frac{\partial F_d}{\partial Y_D} \frac{\partial F_d}{\partial Y_\mu} + \frac{\partial Y_\mu}{\partial \mu} \left( \frac{\partial F_d}{\partial Y_\mu} \right)^2}
\end{aligned} \tag{29}$$

Combining equations (18), (22), (23), (25), (26) and (29), the effective instantaneous tangent modulus tensor is derived instead as

$$\mathbf{C}^{ep} = \mathbf{M}^{T,-1} : \mathbf{U}^{T,-1} : \mathbf{C}_0^{ep} : \mathbf{M}^{T,-1} \tag{30}$$

where

$$\begin{aligned}
\mathbf{U} &= \mathbf{I} - \left( \mathbf{U}_0 + \mathbf{C}_0^{ep} : \mathbf{M}^{T,-1} : \mathbf{U}_0 : \mathbf{M}^{T,-1} : \mathbf{C}^{-1} \right) : \sigma : \mathbf{T} : \mathbf{M}^{T,-1} \\
\mathbf{U}_0 &= \frac{\partial \mathbf{M}}{\partial D} \frac{\partial F_d}{\partial Y_D} + \frac{\partial \mathbf{M}}{\partial \mu} \frac{\partial F_d}{\partial Y_\mu}
\end{aligned} \tag{31}$$

In addition, the derivatives in equations (29) and (31) are derived as

$$\frac{\partial Y_D}{\partial \sigma} = -\frac{2}{1-D} \mathbf{C}^{-1} : \sigma \quad \frac{\partial Y_\mu}{\partial \sigma} = -\frac{2}{1-D} \mathbf{Z} : \sigma \tag{32}$$

$$\frac{\partial Y_D}{\partial D} = \frac{3}{1-D} Y_D \quad \frac{\partial Y_D}{\partial \mu} = \frac{\partial Y_\mu}{\partial D} = \frac{2}{1-D} Y_\mu \quad \frac{\partial Y_\mu}{\partial \mu} = -\sigma^\top : \frac{\partial \mathbf{M}}{\partial \mu} : \mathbf{C}_0^{-1} : \frac{\partial \mathbf{M}}{\partial \mu} : \sigma \tag{33}$$

$$\frac{\partial F_d}{\partial Y_D} = \frac{Y_D}{2Y_d} \quad \frac{\partial F_d}{\partial Y_\mu} = \frac{\gamma Y_\mu}{2Y_d} \tag{34}$$

$$\frac{\partial \mathbf{M}}{\partial \mu} = \frac{1}{1-D} \begin{bmatrix} 0 & 1 & 1 & 0 & 0 & 0 \\ 1 & 0 & 1 & 0 & 0 & 0 \\ 1 & 1 & 0 & 0 & 0 & 0 \\ 0 & 0 & 0 & -1 & 0 & 0 \\ 0 & 0 & 0 & 0 & -1 & 0 \\ 0 & 0 & 0 & 0 & 0 & -1 \end{bmatrix} \quad \frac{\partial \mathbf{M}}{\partial D} = \frac{1}{1-D} \mathbf{M} \quad (35)$$

$$\mathbf{M}^{-1} = (I - D) \begin{bmatrix} m_1 & m_2 & m_2 & 0 & 0 & 0 \\ m_2 & m_1 & m_2 & 0 & 0 & 0 \\ m_2 & m_2 & m_1 & 0 & 0 & 0 \\ 0 & 0 & 0 & m_1 - m_2 & 0 & 0 \\ 0 & 0 & 0 & 0 & m_1 - m_2 & 0 \\ 0 & 0 & 0 & 0 & 0 & m_1 - m_2 \end{bmatrix} \quad (36)$$

$$m_1 = \frac{1 + \mu}{1 + \mu - 2\mu^2} \quad m_2 = -\frac{\mu}{1 + \mu - 2\mu^2}$$

Usually the matrix form of  $\mathbf{C}^{ep}$  in the equation (30) is a 6x6 asymmetric matrix for which most general purpose finite element programs may encounter computational convergency difficulties. Consequently, the symmetric form

$$\mathbf{C}^s = \frac{1}{2} (\mathbf{C}^{ep} + \mathbf{C}^{ep,T}) \quad (37)$$

is taken as a tangent modulus matrix when the finite element stiffness matrix is computed

$$\mathbf{K} = \int_v \mathbf{B}^T : \mathbf{C}^s : \mathbf{B} \quad (38)$$

where  $\mathbf{B}$  is the transformation matrix.

### Crack Initiation Angles for Al 2024-T3 Plates

A thin plate of aluminum alloy 2024-T3 containing an isolated crack was investigated first as shown in Fig.1. The length dimension  $L$  is 86 mm, the thickness of the plate is 3.175 mm and the crack length is 15 mm.  $\theta$  is the inclined angle of the isolated crack and  $\beta$  is the angle measured from the pre-crack direction. Different values of  $\theta$ , namely  $0^\circ$ ,  $30^\circ$ ,  $45^\circ$  and  $60^\circ$ , are chosen for numerical simulation with ABAQUS (Version 5.8). Linear, reduced-integration solid elements are used for the FE analysis. A typical finite element discretization of the plate with a

typical inclined crack of  $45^{\circ}$  is depicted in Fig. 2. Radial elements were chosen around the crack tip for the convenience of determining angular distributions of overall damage at the crack tip. The mechanical properties of AL024-T3, which were determined and reported in reference [10], are summarized as:

$$\begin{array}{lll} E_0=74300 \text{ MPa} & \nu_0=0.34 & R_0=330 \text{ MPa} \\ \gamma=-0.4 & B_0=0.936 \text{ MPa} & w_c=0.185 \end{array}$$

The overall damage distribution in the plate containing a typical inclined crack of  $45^{\circ}$  was calculated as shown in Fig. 3. It can be observed from the figure that the damage accumulation is confined around the crack tip region. Crack initiation is postulated to occur at the location when the overall damage reaches its critical value. The direction of the crack extension  $\beta_i$  is determined from the detailed damage distribution at the crack tip. The angular distributions of the overall damage at the crack tip are calculated as shown in Fig. 4 for different inclined cracks of  $0^{\circ}$ ,  $30^{\circ}$ ,  $45^{\circ}$  and  $60^{\circ}$ . The normalized damage at a constant radial distance from the crack tip was plotted against the angle of rotation  $\beta$ . The location of unit value of the normalized damage is used to determine the direction of crack extension (i.e. the initiation angle  $\beta_i$ ).

Table 1 summarizes the predicted crack initiation angles for the mixed mode specimens. The measured and predicted results based on an anisotropic damage model reported by Chow and Wang are also included for comparison [8]. It can be observed from the table that both of the numerical results agree well with the measured ones. An advantage of the proposed damage model is its ease of computation relative to the anisotropic damage model with a second-order tensor.

### Fracture Analysis for Particulate Composite Plates

The boundary between the particles and the matrix in particulate composites constitutes the source of micro-defects, which will grow and coalesce until a macro-crack is formed under load. To ignore these micro-structural changes in the failure prediction by the conventional methods is not therefore considered realistic. The material deterioration due to damage accumulation should be taken into account for durability analysis with the theory of damage mechanics. The proposed damage model is accordingly applied to predict mixed mode fracture of a thin plate made of a particulate composite as shown in Fig.1. The dimensions of the plate are 4 in.  $\times$  4 in.  $\times$  0.2 in. The length of pre-crack is 1 in. and its inclined angle is represented by  $\theta$ .

In order to determine mechanical properties and damage parameters for the particulate composite material, a modified dog-bone specimen is chosen for the measurement. The specimen is incrementally loaded at different strains until final rupture. Upon each incremental maximum strain, the specimen is unloaded to zero-stress, forming a hysteretic loop. The effective Young's modulus is determined after each unloading. The change of effective Young's modulus is taken as material degradation to evaluate the damage variable  $D$  as shown in Figs. 5 and 6. The true stress-true strain curve of the material is depicted in Fig. 7. The value of  $D_c$ , which is considered an intrinsic material property, was determined to be 0.3. For the particulate composite, the value of Poisson's ratio is assumed to be constant during loading process.

Accordingly, both the damage evolution coefficient  $\gamma$  and the damage variable  $\mu$  are considered insignificant and thus assumed to be zero. Therefore, the damage model is simplified to the conventional isotropic damage model with one scalar damage variable.

The FE analysis is similar to the case example of AL2024-T3. The loading is applied through the displacement boundary condition. The element is postulated to be fully damaged and therefore failed when the plastic damage  $D$  at its integration point reaches a critical value  $D_c$ . The load applied at  $D_c$  is determined as crack initiation load and the position of damaged integration point is used to define the direction of crack extension, i.e. the crack initiation angle. Three different inclined crack angles,  $\theta = 0^\circ$ ,  $30^\circ$  and  $60^\circ$ , are chosen for the analysis. The numerical results on the crack initiation angle and the fracture load are summarized in Tables 2 and 3, demonstrating a satisfactory agreement with the experimental measurements.

### Summary

Damage-coupled finite element formulation has been derived for the proposed damage model. The model has been implemented in ABAQUS (version 5.8) through its UMAT subroutine for failure analysis of mixed mode fracture. A failure criterion is developed to determine the crack initiation at the location where the overall damage accumulation reaches a critical value of the material. Therefore, the crack initiation angle and fracture load can be determined from the FEM results. Two engineering materials, AL2024-T3 and a particulate composite, are chosen for the investigation. A mixed mode fracture analysis was carried out and the predicted results are compared well with the test data.

### References

1. Giovanola, J.H. and Finnie, I., (1984): "A review of the Use of the J-Integral as a Fracture Parameter", *SM Archives*, Vol. 9, pp. 197-225.
2. Giovanola, J.H. and Finnie, I., (1984): "The Crack-Opening Displacement (COD) as a Fracture Parameter and a Comparative Assessment of the COD and J-Integral Concepts", *SM Archives*, Vol. 9, pp. 227-257.
3. Liu, H.W. and Zhuang, T., (1985): "A Dual Parameter Elastic-Plastic Fracture Criterion", *International Journal of Fracture*, Vol. 27, pp. R87-91.
4. Kachanov, L.M., (1958): "On Creep Rupture Time", *Izv. Acad. Nauk SSSR Otd, Techn. Nauk*, Vol. 8, pp. 26-31.
5. Lemaitre, J. and J. L. Chaboche, (1990): *Mechanics of Solid Materials*, Cambridge University Press.
6. Krajcinovic, D. and J. Lemaitre, (1987): *Continuum Damage Mechanics Theory and Applications*, International Center for Mechanical Sciences Courses and Lectures, No. 295, Springer, Berlin.
7. Chow, C.L. and Wang, J., (1988): "Ductile Fracture Characterization with an Anisotropic Continuum Damage Theory", *Engineering Fracture Mechanics*, Vol. 30, pp. 547-563.
8. Chow, C.L. and Wang, J., (1989): "On Crack Initiation Angle of Mixed Mode Ductile Fracture with Continuum Damage Mechanics", *Engineering Fracture Mechanics*, Vol. 32, pp. 601-612.
9. Chow, C.L. and Wang, J., (1989): "Crack Propagation in Mixed-Mode Ductile Fracture with Continuum Damage Mechanics", *Proc Instn Mech Engrs*, Vol. 203, pp. 189-199.

10. Chow, C. L. and Wei, Y., (1999): "Constitutive Modeling of Material Damage for Fatigue Failure Prediction", *Int. J. Damage Mechanics*, Vol. 8, pp. 355-375.

Table 1 Crack Initiation Angle  $\beta_i$  for Al2024-T3  
(characteristic crack length: 0.1 mm)

inclined angle $\theta$	test	numerical simulation	
		proposed model	anisotropic model
0	0	0	0
30	35.9	37.5	43
45	53.7	52.5	56
60	71.2	67.5	73

Table 2 Crack Initiation Load for Particulate Composite  
(characteristic crack length: 1.4 mm)

Pre-crack angle ( $^{\circ}$ )		0	30	60
Load (lb)	prediction	24.0	27.2	36.9
	test	23.4	27.0	36.2

Table 3 Crack initiation Angle  $\beta_i$  ( $^{\circ}$ ) Particulate Composite  
(characteristic crack length: 1.4 mm)

Pre-crack angle $\theta$ ( $^{\circ}$ )		0	30	60
$\beta_i$ ( $^{\circ}$ )	prediction	0	28	62
	test	0	33	68

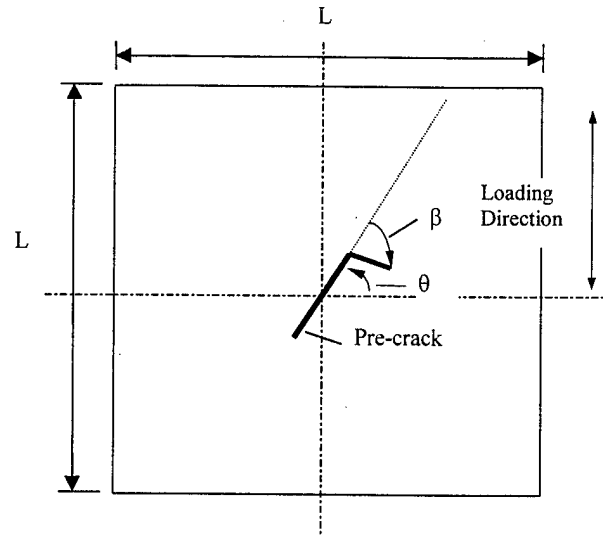


Fig. 1 Mixed mode specimen

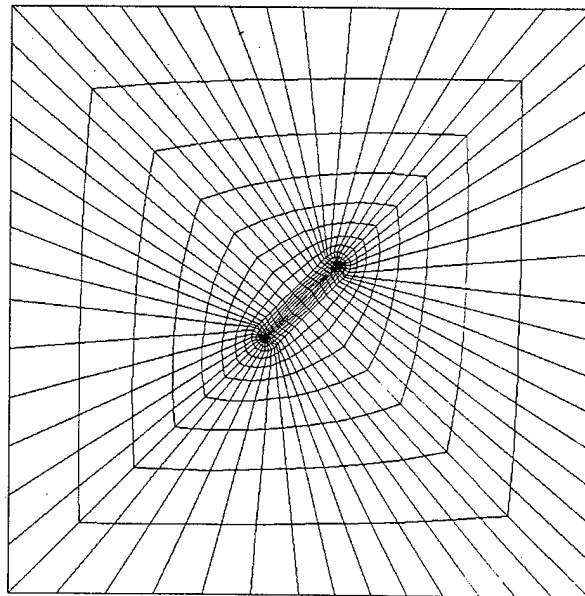


Fig. 2 Typical finite elements for mixed mode fracture analysis

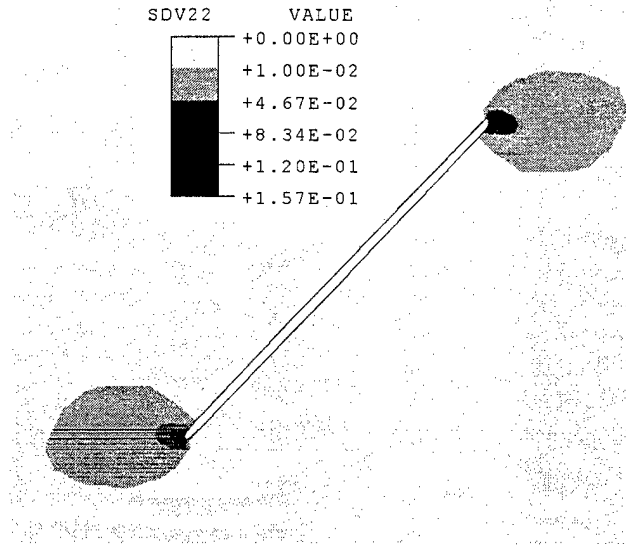


Fig. 3 Damage distribution contours in AL2024-T3 plate for  $\theta = 45^{\circ}$

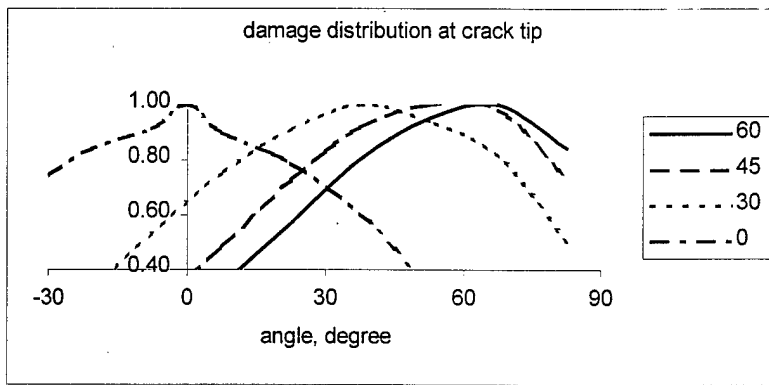


Fig 4 Angular distributions of damage for mixed mode AL2024-T3 specimen

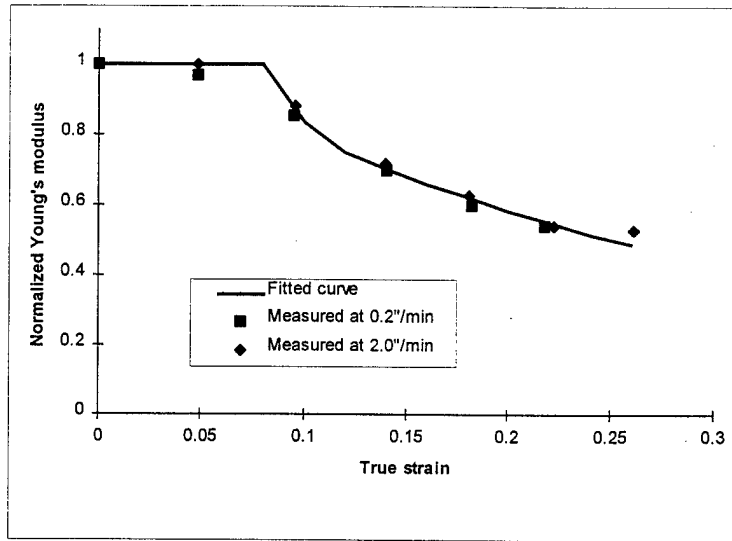


Fig. 5 Normalized Young's modulus vs. applied strain for a particulate composite

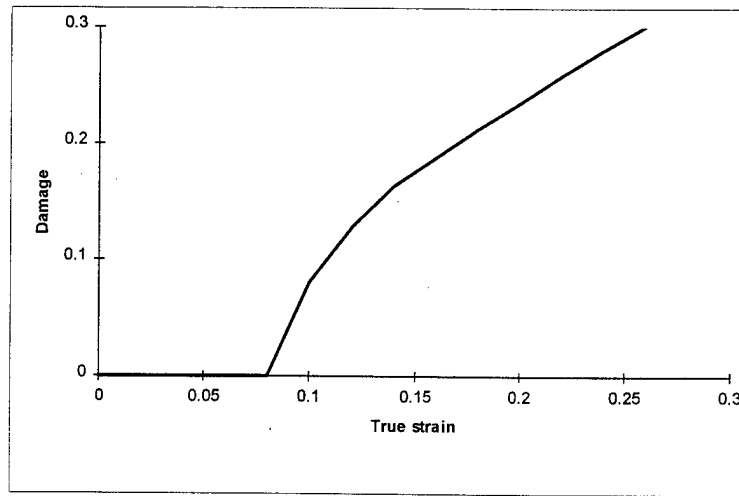


Fig. 6 Damage evolution curve for a particulate composite

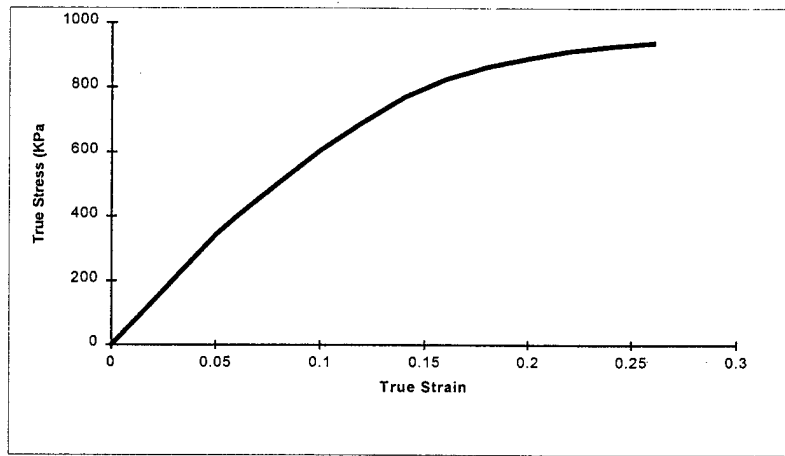


Fig. 7 True stress-true strain curve for a particulate composite